# The Initiation and Early Stages of Postmolt Mineralization in the Blue Crab, *Callinectes sapidus*

*Robert D. Roer\* and Richard M. Dillaman†*

*Department of Biology and Marine Biology, University of North Carolina Wilmington, Wilmington, NC, United States*

Crabs are encased in a rigid exoskeleton or cuticle that is hardened by both protein crosslinking and calcification. In order to grow, the exoskeleton must be periodically molted. The two outermost layers of the exoskeleton of crabs are deposited prior to the molt, but remain uncalcified until the animal sheds its old exoskeleton. The inhibition of premolt calcification and initiation of postmolt calcification are effected by biochemical changes in the organic matrix. In the 2 h after the molt, sugar moieties are enzymatically altered on cuticular glycoproteins by an N-acetylhexosaminidase secreted by the underlying epithelium. These alterations appear to unmask nucleation sites that allow calcification to commence. The initial deposition of mineral is in the form of amorphous calcium carbonate (ACC). As postmolt calcification continues and the principal layer (endocuticle) is deposited and mineralized, the ACC is largely converted to or overgrown by calcite. Prior to the onset of ACC deposition, silicon has been detected in those areas of the exoskeleton that are about to undergo mineralization. As calcification proceeds, silicon is no longer detected. It is hypothesized that silicon is involved in the stabilization of ACC by destabilizing the crystal lattice of calcite before it undergoes the transition to or is overgrown by crystalline calcite.

Keywords: *Callinectes*, molting, calcification, silicon, amorphous calcium carbonate, glycoproteins, N-acetylglycosaminidase

## INTRODUCTION

In the words of Hans Lowenstam and Steve Weiner, "Crustaceans are the champions of mineral mobilization and deposition in the animal kingdom" (Lowenstam and Weiner, 1989). To illuminate and substantiate this claim, we will review work on the cellular and molecular control of biomineralization in decapod crustaceans and present some new preliminary data on the presence and role of silica in this process.

The utility of crustaceans as a model for studying biomineralization lies in the fact that they must molt their calcified exoskeletons periodically in order to grow (Roer and Dillaman, 1984, 1993; Luquet, 2012). The exoskeleton, as typified by the dorsal carapace of decapod crabs, consists of four layers, from the outermost: epicuticle, exocuticle, endocuticle, and membranous layer. The epicuticle contains a protein and lipid-rich organic matrix. The inner three cuticular layers all contain an organic matrix comprised of protein and chitin microfibrils arranged in sheets that parallel the body surface. The orientation of the sheets changes with successive layers, forming a helicoidal arrangement (Bouligand, 1972; Raabe et al., 2005). When fully formed, the outer three layers are impregnated with calcium carbonate in the form of calcite. A unique feature of the

exocuticle is the vertical partitioning of the layer into hexagonal prisms. The prisms are bounded by interprismatic septa which create a honeycomb-like arrangement within this layer (Roer and Dillaman, 1984). The role of the septa in the initial stages of calcification will be discussed below.

The membranous layer is underlain by a hypodermis. The outer cellular layer of the hypodermis is an epithelium that elaborates the exoskeletal layers after each molt and which extends microvilli through all the layers, terminating in the inner epicuticle. The microvilli become encased in cuticular material referred to as pore canals. We have also proposed that the interprismatic septa morphologically correspond to the lateral margins of the epithelial cells that persist following cuticular secretion (Roer and Dillaman, 1984).

The molt cycle is divided into four main stages: Intermolt (stage $C_4$) when the exoskeleton is fully elaborated, premolt (stages $D_0$, $D_1$, $D_2$, $D_3$, $D_4$), ecdysis (stage E), and postmolt (stages $A_1$, $A_2$, $B_1$, $B_2$, $C_{1-3}$) (Drach, 1939; Drach and Tchernigovtzeff, 1967). Premolt is initiated by apolysis, the enzyme-mediated separation of the epithelium from the overlying old cuticle. Late premolt (stage $D_2$) is the period during which resorption of mineral and organic material from the old exoskeleton peaks, along with the synthesis and elaboration of the organic matrix of the new epicuticle and exocuticle. While these "pre-exuvial" layers are fully formed prior to the molt, they remain uncalcified until after the molt to allow for expansion of the new, soft exoskeleton. Just prior to the molt (ecdysis), during stages $D_3$ and $D_4$, preformed sutures along the margin of the old carapace weaken and split open. The crab then emerges from the old exoskeleton (stage E), and enters postmolt (Roer and Dillaman, 1993).

Early postmolt (stages $A_1$ and $A_2$) are characterized by sclerotization of the pre-exuvially deposited epi- and exocuticle, and within 3 h after the molt, the initiation of calcification of these layers (Shafer et al., 1995). Mineralization begins along the epicuticle, the inner and outer edges of the exocuticle, and at the distal and proximal margins of the interprismatic septa. Calcification of the septa continues until the mineralization fronts meet between 5 and 8 h after ecdysis. At this point the pattern of mineralization resembles corrugated cardboard, lending early stability and strength to the exoskeleton (Dillaman et al., 2005).

The mineral that is first deposited along the septa and exocuticular margins is amorphous calcium carbonate (ACC). This is evident by the high solubility of the initial mineral (Dillaman et al., 2005). This labile mineral persists along the outer and inner exocuticular margins and interprismatic septa through 12 h postecdysis. By 48 h postmolt, as mineralization continues, the ACC is no longer observed and was presumed to be transformed to calcite (Dillaman et al., 2005).

During the late postmolt stages B and $C_{1-3}$, mineralization of the exocuticle within the prisms continues along with the concurrent deposition and calcification of the endocuticle. Termination of exoskeletal deposition and mineralization are marked by the secretion of the non-calcified membranous layer, signaling the transition to intermolt (stage $C_4$) (Roer and Dillaman, 1993; Dillaman et al., 2005).

Premolt resorption of calcium from the old exoskeleton is mediated by Ca-ATPase and Na/Ca exchangers localized along the basolateral membranes of the epithelial cells (Roer, 1980; Greenaway et al., 1995). Postmolt translocation of calcium from the hemolymph into the new cuticle is also accomplished by the same transporters, but now they are localized to the apical cell membranes and the microvilli that extend into the cuticle via the pore canals (Roer, 1980; Greenaway et al., 1995; Roer and Towle, 2005). Bicarbonate transport into the mineralizing exoskeleton involves carbonic anhydrase and a $HCO_3$-ATPase (Roer and Dillaman, 1993).

The sequence of events during the molt cycle described above clearly demonstrates why decapod crustaceans are such a valuable model for studying the mechanisms and control of mineralization. It also poses questions that have been the subject of intense study in our research group over the past few decades. The first of these is how the pre-exuvial layers are prevented from calcifying prior to the molt and then promoted to initiate mineralization within 2 h after ecdysis.

The control of mineralization in the pre- and postmolt cuticle resides in the biochemistry of the organic matrix. Samples of cuticle, devoid of epithelium, from pre-exuvial epi- and exocuticle are incapable of forming calcite crystals in vitro. However, decalcified early postmolt epi- and exocuticle samples nucleate crystal formation under identical conditions (Roer et al., 1988). This change in the ability of the matrix to support calcification temporally and spatially corresponds to changes in the profiles of glycoproteins within the cuticle. Marlowe et al. (1994) demonstrated the changes in the sugar moieties within the cuticle histologically, using labeled lectins. Shafer et al. (1994, 1995) characterized the change in sugar moieties on individual glycoproteins and demonstrated that these changes coincided with the alteration of the cuticle's ability to nucleate mineral deposition.

A causal relationship was first established by Coblentz et al. (1998) using a pH-drift in vitro mineralization assay. Protein extracts from pre-exuvial exocuticle had no effect on calcite precipitation, but acetic acid extracts of cuticle 1.5 or more hours postecdysis were found to bind to nascent calcite crystals and inhibit nucleation. These data suggest that two proteins in postecdysial cuticle, when fixed to the chitin protein fibrils act as nucleation sites, but these proteins are shielded prior to the postmolt transition in the cuticle.

The hypothesis that the shielding of the nucleating glycoproteins involved one or more sugar moieties was suggested by the discovery of a glycosidase extracted from postecdysial cuticle with both N-acetylglucosaminidase and N-acetylgalactosaminidase activity (Roer et al., 2001). A partial sequence of this putative cuticular N-acetylhexosaminidase was determined (Roer and Towle, 2004). The potential role for this enzyme in mediating the onset of nucleation was supported by experiments in which pre-exuvial cuticle was treated with an exogenous N-acetylhexosaminidase (Pierce et al., 2001). The untreated pre-exuvial cuticle was incapable of nucleating calcite in vitro. However, after treatment with the N-acetylhexosaminidase, the pre-exuvial cuticle nucleated calcite deposition as well as postmolt cuticle samples did.

Faircloth and Shafer (2007) were able to identify cuticular proteins that are likely to be involved in biomineralization by comparing transcripts that were found in calcifying dorsal carapace tissue of the blue crab to transcripts that were only found in the tissue underlying the arthrodial membrane of the joints which doesn't mineralize. Four transcripts found only in arthrodial membrane tissue (CsAMP's) all contained the Rebers-Riddiford motif (RR-1) that is a chitin-binding sequence. One of these, CsAMP9.3 was concluded to code for a structural element of the exocuticle, since it was only detected in premolt tissue (the stage when exocuticular synthesis occurs). Of the four transcripts isolated from calcifying tissue, two (CsCP6.1 and CsCP19.0) are only expressed during postmolt, suggesting that they may be involved with the calcification of the endocuticle, while a third (CsCP15.0) is expressed in both pre- and postmolt. The fourth (CsCP14.1) also possessed the RR-1 motif and was only expressed during pre-molt. It was hypothesized that CsCP14.1 binds to chitin-protein fibrils during premolt and prevents pre-exuvial nucleation of $CaCO_3$, and that CsCP6.1 is expressed during postmolt to initiate mineralization.

Tweedie et al. (2004) isolated a glycoprotein from blue crab exocuticle and created an antibody to it. They employed immunohistochemistry to localize the glycoprotein *in situ*. The glycoprotein was widely distributed in the exocuticle immediately after the molt, but at the time that calcification began (∼1.5 h postecdysis), the glycoprotein disappeared from the interprismatic septa. Thus, its disappearance corresponded temporally and spatially to the nucleation of $CaCO_3$. It was hypothesized that this glycoprotein was involved in preventing pre-exuvial mineralization of the exocuticle.

Kuballa and Elizur (2008) characterized two cuticular proteins from the crab *Portunus pelagicus*, a C-type lectin receptor that was up-regulated in premolt and a mannose-binding protein that was only expressed postmolt. They hypothesized that the former was involved in inhibiting pre-exuvial calcification and the latter in promoting postmolt mineralization. A more detailed discussion of proteins that are potentially involved with the initiation and control of mineralization in decapod crustaceans can be found in Roer et al. (2015).

Another question raised by our previous work regards the presence of ACC during the early stages of postmolt calcification. Over the past few decades, it has been shown that numerous mineralized structures across a wide array of taxa display a transient, amorphous phase prior to the appearance of the crystalline phase (Addadi et al., 2012). The problem is that amorphous phases are very unstable and, at least in the case of $CaCO_3$, generally undergoes nearly instantaneous transition to crystalline calcite or aragonite. How ACC is stabilized for rather prolonged periods during early premolt in the blue crab has not been explained. There is, however, evidence in the cystoliths from an angiosperm (*Morus alba*) and synthetic ACC, that the amorphous phase is stabilized by the presence of silicate (Gal et al., 2010). The possible mechanism for ACC stabilization proposed by Gal et al. (2010) is "geometric frustration" of the calcite crystal lattice. The calcite lattice is characterized by a planar arrangement of carbonate ions. It is hypothesized that the relatively large tetrahedral silicate ion, with four negative charges, would both interrupt the lattice and the charge equilibrium at the crystal surface.

It has also been reported that silicon is either involved in the process of calcification (coccolithophorids, Durak et al., 2016) or is detected at the initial sites of calcification in bone (Carlisle, 1970; Landis et al., 1986), brachiopod shell (Williams et al., 2001), cyanobacteria and isopod crustacean exoskeletons (Matsko et al., 2011). In the latter study, silicon was localized in the region of the mineralizing cuticle where calcite would subsequently be found.

To determine if silicon is present during the initial stages of mineralization in the blue crab and if it might play a role in stabilizing ACC in early premolt, we undertook the present study. We employed scanning electron microscopy with energy-dispersive analysis of X-rays (EDAX) to compare the distribution and the relative amounts of Ca and Si in relation to the patterns of initial mineralization. We employed both the dorsal carapace, which mineralizes, and (as a control) the arthrodial membrane of the joints, which never calcifies. Both tissues were sampled from animals in both premolt and early postmolt. If Si plays a role in calcification, we would expect to find it associated with the sites of the initial stages of mineralization (i.e., early postmolt) in the carapace, but absent or less prevalent in the non-mineralizing arthrodial membrane.

## MATERIALS AND METHODS

Samples of the dorsal carapace (from above the cardiac region) and arthrodial membrane (from between the merus and carpus of the chelipeds) were dissected from 18 blue crabs (*Callinectes sapidus*; Rathbun, 1896), six from each of the following molt stages: $D_3$, $A_1$, and $A_2$. Molt stages were determined according the criteria of Drach (1939) and Drach and Tchernigovtzeff (1967). Crabs were obtained at Endurance Seafood, a commercial crab shedding operation in Colington, NC, and locally in Wilmington, NC. Samples were fixed and stored in 95% ethanol.

Samples across all molt stages were prepared for scanning electron microscopy (SEM) analysis. For late premolt (stage $D_3$), the old and new cuticle separate on dissection and only the new, pre-exuvial cuticle was used. Samples were trimmed with a razor blade, and dehydrated using two, 20-min-long changes of 100% ethanol, followed by two 20-min-long changes of 1:1 propanol:ethanol and two 20-min-long changes of 100% propanol. After dehydration these samples were left to air dry overnight. All samples were then mounted on aluminum stubs (Ted Pella Prod. No. 16111) with a carbon adhesive (Ted Pella Prod. No. 16084-1) and coated with 10-nm of platinum/palladium (Pt/Pd) alloy in a Cressington 208HR sputter coater.

All imaging was performed on a Phillips XL30-S FEG system running the software program Microscope Control version 6.0. Secondary electron micrographs were collected using a working distance of 7.5 mm, beam strength of 5 Kev, and spot size 3. Energy dispersive X-ray analysis (EDAX) (beam strength 25 Kev,

spot size 4, working distance of 7.5 mm) was used to analyze the chemical composition of the embedded tissue samples. X-ray emission spectra were obtained using the program EDX Control version 3.3 with a dead time of approximately 20% and counts per second above 1500 for a total of 200 live seconds; the spatial distribution of the identified significant peaks was mapped using program EDX Map version 3.3. Semi-quantitative compositional analysis to determine relative proportions by weight percent of each element in the sample was obtained through the "Quantify" function in EDX Control including all identified significant peaks. Compensation for sample-to-sample variations due to differences in surface features or orientation were accomplished by using the ratios of Ca and Si to each other and to Pt, which was applied at the same thickness to all samples and therefore could be used as a reference.

## RESULTS

SEM examination of samples from the dorsal carapace just before ecdysis (stage $D_3$), those just after the molt (stage $A_1$), and those taken 6 h postmolt (stage $A_2$) showed no differences in cuticular thickness, nor any gross morphological differences. The fiber and lamellar structure of the exocuticle became more apparent after the molt, as did the vertical structural elements of the epicuticle. The structure of the arthrodial membrane cuticle showed similar morphological characteristics and differed most markedly from that of the dorsal carapace in that the former was approximately two-thirds the thickness of the latter (**Figure 1**).

Elemental mapping of Ca and Si across the $D_3$ dorsal carapace samples showed a sparse and homogeneous distribution of both elements across the entire expanse of the epi- and exocuticle. This was the same pattern observed in all premolt and postmolt arthrodial membrane cuticle samples. In the dorsal carapace samples at stage $A_1$, the Si distribution was still rather homogeneous, but observably denser than during premolt. The Ca signal was also far more intense, but also was no longer homogeneously distributed. Instead, there was a more intense Ca signal on the outer surface of the cuticle and throughout the exocuticle. Less Ca was seen within the epicuticle, than in the exocuticle (**Figure 1**).

Stage $A_2$ dorsal carapace samples showed a decrease in both the density and homogeneity of the Si signal relative to stage $A_1$. The Ca signal showed a very high intensity at the outer and inner margins of the exocuticle, corresponding to areas of initial mineralization at this stage. The Ca+Si composite (**Figure 1**, rightmost column) showed that the Si distribution appeared to be more highly localized to those areas that had not yet begun to calcify—the epicuticle and mid-region of the exocuticle.

The quantitative data support the observations based on the EDAX elemental maps (**Figure 2**). Whether viewed as a straight atomic % or relative to the reference atomic % of Pt, the arthrodial membrane cuticle showed immeasurably low levels of Si, and very low levels of Ca throughout early postmolt (**Figures 2A,B**). In premolt, pre-exuvial carapace cuticle, there were very low levels of both Ca and Si (**Figures 2A,B**), and the

levels of each element were very close to the same, as shown in their atomic % ratios (**Figures 2C,D**).

In postmolt carapace samples, it appeared that as the atomic % of Ca increased, there was a concomitant decrease in the atomic % of Si. There was considerable variation between samples in early premolt (stage $A_1$). The sample from crab #6 (A1 C-6 in **Figures 2A,B**) had levels that were intermediate to those from premolt (sample D3 C-3) and a different early postmolt sample from crab #1 (A1 C-1). The latter showed levels of Ca and Si very similar to the representative stage $A_2$ sample (A2 C-3) (**Figures 2A,B**). The Ca/Si ratio increased (and Si/Ca decreased) as mineralization commenced during postmolt (**Figures 2C,D**).
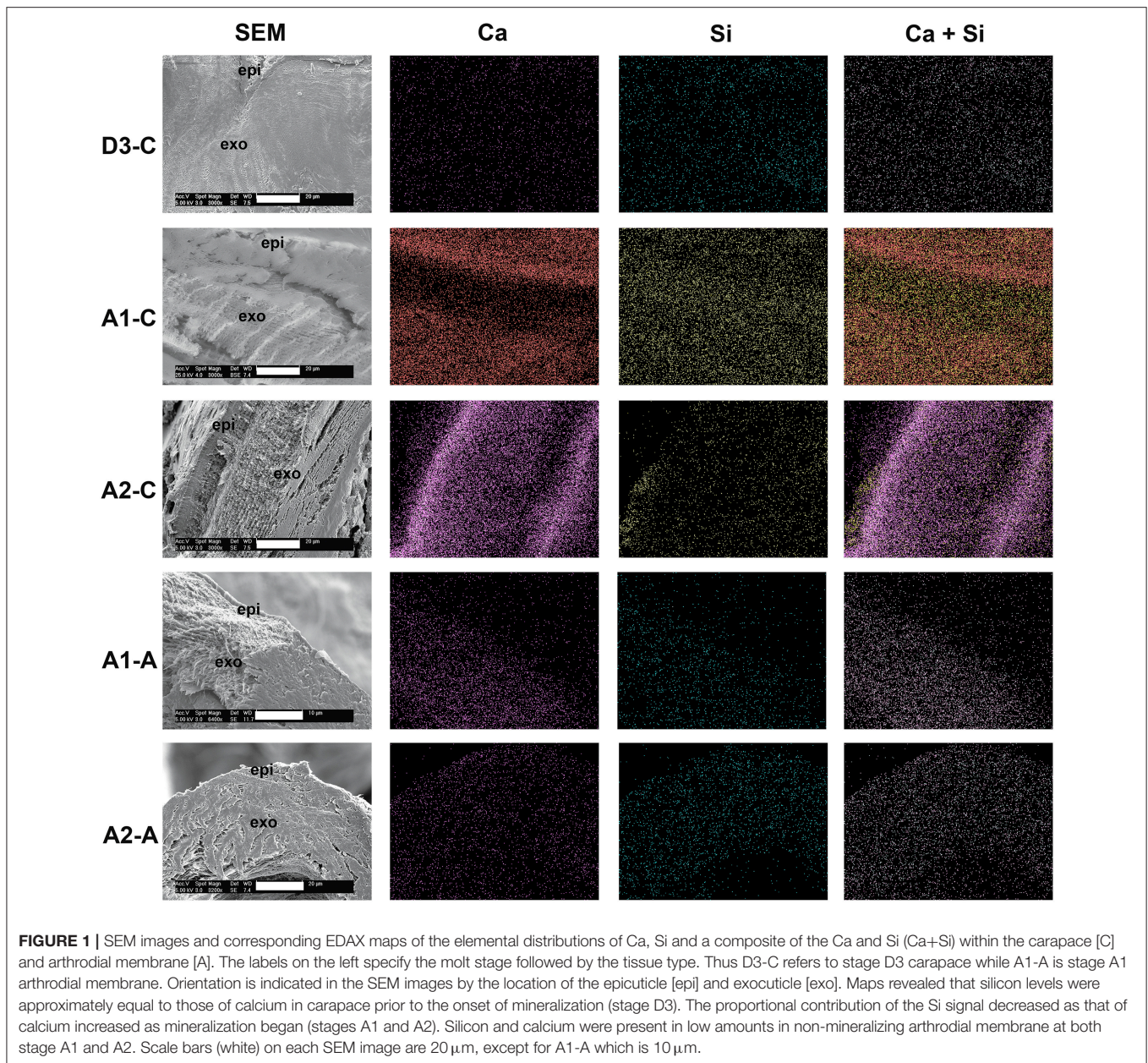
## DISCUSSION

Interest in the involvement of Si in biomineralization in Crustacea is not new. Reports of silicified mandibles have been reported in copepods (Beklemishev, 1954; Miller et al., 1990; Michels et al., 2012; Michels and Gorb, 2015) and amphipods (Mekhanikova et al., 2012). More recently we described silicified teeth in the gastric mill of the blue crab (Vatcher et al., 2015; Nesbit and Roer, 2016). However, an association of Si with calcification in crustaceans has only been suggested by one study on the isopod *Ligia italica* (Matsko et al., 2011). Matsko and colleagues detected the presence of Si in the developing, unmineralized matrix of the exocuticle at the margins of the chitin-protein fibrils. These corresponded precisely to the sites where calcite would be later located in the mature cuticle. The authors hypothesized that Si may form a bridge between the chitin-protein fibrils and the calcium minerals, acting as a nucleation site.

The present study also found Si to be present prior to the onset of mineralization, but its distribution was more homogeneous that that observed by Matsko et al. (2011). Si, presumably in the form of silica, was found diffusely throughout the dorsal carapace exocuticle during late premolt. Ca was also present at similarly low and diffuse levels in this tissue prior to ecdysis. After the molt, Ca concentration increased markedly through stage $A_1$, as evidenced by the two examples presented in **Figure 2**. Just after the molt, Si appeared to increase (A1 C-6 in **Figure 2A**). While this could possibly be due to a decrease in other elements, thereby increasing the % atomic composition of Si, the increase in the ratio of Si to Pt (**Figure 2B**) argues for an actual increase in Si content.

As stage $A_1$ progresses to stage $A_2$, there was a sharp increase in Ca concentration. This corresponds both spatially and temporally to the initial deposition of $CaCO_3$ along the inner and outer exocuticular margins (Dillaman et al., 2005). Concomitant with the increase in Ca was a decrease in the Si signal (**Figure 2A**). Again, this could have been due to the increase in Ca atomic % which would make Si have a relatively lower atomic %. However, the Si to Pt ratio also decreases markedly suggesting that there is an actual decrease in the amount of Si in the exoskeleton (**Figure 2B**).
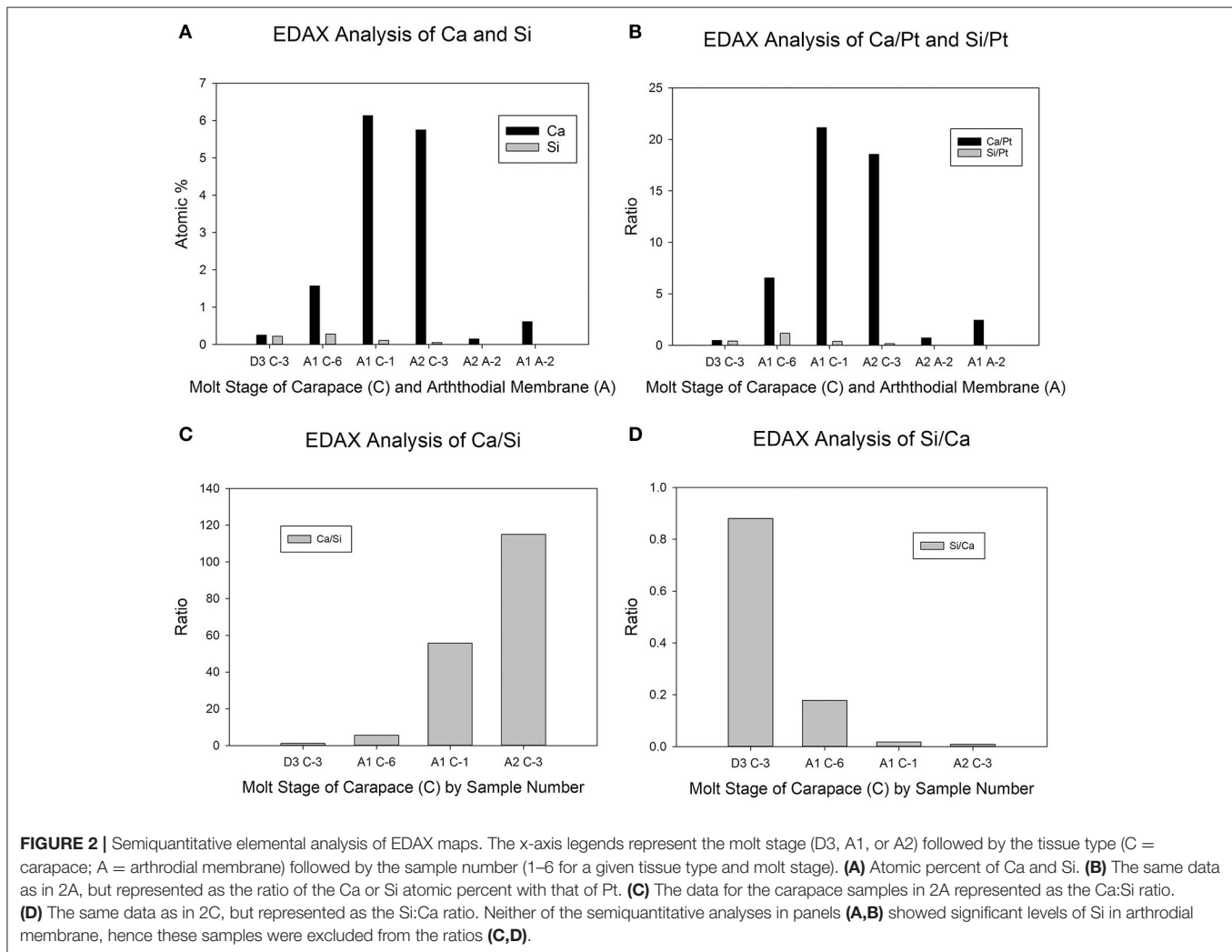
We hypothesize that Si plays some role in calcification since Si is only present to a detectable level in the mineralizing tissue and

**FIGURE 1 |** SEM images and corresponding EDAX maps of the elemental distributions of Ca, Si and a composite of the Ca and Si (Ca+Si) within the carapace [C] and arthrodial membrane [A]. The labels on the left specify the molt stage followed by the tissue type. Thus D3-C refers to stage D3 carapace while A1-A is stage A1 arthrodial membrane. Orientation is indicated in the SEM images by the location of the epicuticle [epi] and exocuticle [exo]. Maps revealed that silicon levels were approximately equal to those of calcium in carapace prior to the onset of mineralization (stage D3). The proportional contribution of the Si signal decreased as that of calcium increased as mineralization began (stages A1 and A2). Silicon and calcium were present in low amounts in non-mineralizing arthrodial membrane at both stage A1 and A2. Scale bars (white) on each SEM image are 20 μm, except for A1-A which is 10 μm.

is absent at all stages observed in the non-calcifying arthrodial membrane cuticle. The function of Si in the earliest stages of CaCO$_3$ deposition has not been determined. Studies on other systems have suggested some possible roles.

Durak et al. (2016) found that some species of coccolithophores (*Coccolithus braarudii*, *Calcidiscus leptoporus*, *Scyphosphaera apsteinii*) possess a Na$^+$-coupled high-affinity Si transporter (SIT) or SIT-like transporter similar to that found in silicifying diatoms. SITs are competitively inhibited by germanium. They discovered that incubating these species of coccolithophores in the presence of Ge inhibited calcification and caused malformed coccoliths to be produced.

Silica has been implicated in the early stages of the mineralization of a variety of calcified tissues, potentially involved in either the synthesis of organic matrix components or in the nucleation of the calcium minerals. Silicates were observed in the pre-mineralized osteoid in bones of chicks, mice and rats (Carlisle, 1970; Landis et al., 1986). There is evidence that Si may be a necessary factor in the synthesis of collagen and can promote osteoblast proliferation and activity. The larval shell of the brachiopod, *Discinisca*, is mineralized by the formation of siliceous tablets. However, when the larva settles, the mantle epithelium begins to deposit apatite. Williams et al. (2001) hypothesized that the silica catalyzed the precipitation of apatite.

**FIGURE 2 |** Semiquantitative elemental analysis of EDAX maps. The x-axis legends represent the molt stage (D3, A1, or A2) followed by the tissue type (C = carapace; A = arthrodial membrane) followed by the sample number (1–6 for a given tissue type and molt stage). **(A)** Atomic percent of Ca and Si. **(B)** The same data as in 2A, but represented as the ratio of the Ca or Si atomic percent with that of Pt. **(C)** The data for the carapace samples in 2A represented as the Ca:Si ratio. **(D)** The same data as in 2C, but represented as the Si:Ca ratio. Neither of the semiquantitative analyses in panels **(A,B)** showed significant levels of Si in arthrodial membrane, hence these samples were excluded from the ratios **(C,D)**.

Matsko et al. (2011) also proposed that Si binds to N-acetyl-glucosamine (the monomer of chitin) to attract bicarbonate ions and serve as nucleation sites for calcium carbonate precipitation.

Gal et al. (2010) have produced definitive data on the ability of Si to stabilize ACC. They compared the temperature stability of ACC in the cystoliths in the leaves of two angiosperms, *Ficus microcarpa* and *M. alba*. In both species, the cystoliths retain ACC throughout the life of the leaf *in vivo*. Elemental mapping showed no evidence of Si associated with the ACC phase in *F. microcarpa*, but a small Si peak in the cystolith ACC of *M. alba*. The isolated cystolith ACC will crystalize to calcite *in vitro* upon heating as the hydrated ACC loses its bound water. The authors demonstrated that the ACC from *F. microcarpa* crystallized at a significantly lower temperature than that from *M. alba*, suggesting that the presence of Si stabilized the ACC. The authors confirmed this hypothesis by creating synthetic ACC with varying Si content. The greater the Si content, the higher the transition temperature at which ACC crystalized to calcite.

The temporal and spatial distribution of Si and Ca in the postmolt dorsal carapace cuticle of the blue crab are consistent with this hypothesis of ACC stabilization. The concentration and distribution of Si were highest at the time and region of initial calcification in the new exocuticle. The initial phase of the mineral deposition in these regions is ACC (Dillaman et al., 2005). The level of Si decreased at the time (stage A$_2$) when ACC transforms to calcite. The crustacean exoskeleton presents an excellent model in which to further investigate this hypothetical framework as well as other aspects of biomineralization.

## ETHICS STATEMENT

The study was exempt from the above requirements in that it only utilized invertebrate organisms.

## AUTHOR CONTRIBUTIONS

Both authors made substantial, direct and intellectual contributions to the work. The manuscript was written by RR after the death of RD.

## ACKNOWLEDGMENTS

## REFERENCES

Addadi, L., Vidavsky, N., and Weiner, S. (2012). Transient precursor amorphous phases in biomineralization. In the footsteps of Heinz A. *Lowenstam. Z. Kristallogr.* 227, 711–717. doi: 10.1524/zkri.2012.1524

Beklemishev, K. V. (1954). The discovery of siliceous formations in the epidermis of lower crustaceans. *Dokl. Akad. Nauk. SSSR* 3, 543–545.

Bouligand, Y. (1972). Twisted fibrous arrangements in biological materials and cholesteric mesophases. *Tissue Cell* 4, 189–190, 192–217. doi: 10.1016/S0040-8166(72)80042-9

Carlisle, E. M. (1970). Silicon: a possible factor in bone calcification. *Science* 167, 279–280. doi: 10.1126/science.167.3916.279

Coblentz, F. E., Shafer, T. H., and Roer, R. D. (1998). Cuticular proteins from the blue crab alter *in vitro* calcium carbonate mineralization. *Comp. Biochem. Physiol.* 121B, 349–360. doi: 10.1016/S0305-0491(98)10117-7

Dillaman, R., Hequembourg, S., and Gay, M. (2005). Early pattern of calcification in the dorsal carapace of the blue crab, *Callinectes sapidus. J. Morphol.* 263, 356–374. doi: 10.1002/jmor.10311

Drach, P. (1939). Mue et cycle d'intermue chez les crustacés décapodes. *Ann. Inst. Oceanogr.* 19, 103–391.

Drach, P., and Tchernigovtzeff, C. (1967). Sur la méthode de détermination des stades d'intermue et son application générale aux crustaces. *Vie Milieu* 18, 595–610.

Durak, G. M., Taylor, A. R., Walker, C. E., Probert, I., de Vargas, C., Audic, S., et al. (2016). A role for diatom-like silicon transporters in calcifying coccolithophores. *Nat. Commun.* 7:10543. doi: 10.1038/ncomms10543

Faircloth, L. M., and Shafer, T. H. (2007). Differential expression of eight transcripts and their roles in the cuticle of the blue crab, *Callinectes sapidus. Comp. Biochem. Physiol.* 146B, 370–383. doi: 10.1016/j.cbpb.2006.11.008

Gal, A., Weiner, S., and Addadi, L. (2010). The stabilizing effect of silicate on biogenic and synthetic amorphous calcium carbonate. *J. Am. Chem. Soc.* 132, 13206–13211. doi: 10.1021/ja106883c

Greenaway, P., Dillaman, R. M., and Roer, R. D. (1995). Quercitin-dependent ATPase activity in the hypodermal tissue of *Callinectes sapidus* during the moult cycle. *Comp. Biochem. Physiol.* 111A, 303–312. doi: 10.1016/0300-9629(94)00205-8

Kuballa, A. V., and Elizur, A. (2008). Differential expression profiling of components associated with exoskeletal hardening in crustaceans. *BMC Genomics* 9:575. doi: 10.1186/1471-2164-9-575

Landis, W. J., Lee, D. D., Brenna, J. T., Chandra, S., and Morrison, G. H. (1986). Detection and localization of silicon and associated elements in vertebrate bone tissue by imaging ion microscopy. *Calcif. Tissue Res.* 38, 52–59. doi: 10.1007/BF02556595

Lowenstam, H. A., and Weiner, S. (1989). *On Biomineralization.* New York, NY: Oxford University Press.

Luquet, G. (2012). Biomineralizations: insights and prospects from crustaceans. *Zookeys* 176, 103–121. doi: 10.3897/zookeys.176.2318

Marlowe, R. L., Dillaman, R. M., and Roer, R. D. (1994). Lectin binding by crustacean cuticle: the cuticle of *Callinectes sapidus* throughout the molt cycle, and the intermolt cuticle of *Procambarus clarkii* and *Ocypode quadrata. J. Crust. Biol.* 14, 231–246. doi: 10.2307/1548904

Matsko, N. B., Znidaršic, N., Letofsky-Papst, I., Dittrich, M., Grogger, W., Strus, J., et al. (2011). Silicon: the key element in early stages of biocalcification. *J. Struct. Biol.* 174, 180–186. doi: 10.1016/j.jsb.2010.09.025

Mekhanikova, I. V., Andreev, D. S., Belozerova, O. Y., Mikhlin, Y. L., Lipko, S. V., Klimenkov, I. V., et al. (2012). Specific features of mandible structure and elemental composition in the polyphagous amphipod *Acanthogammarus grewingkii* endemic to Lake Baikal. *PLoS ONE* 7:e43073. doi: 10.1371/journal.pone.0043073

Michels, J., and Gorb, S. N. (2015). Mandibular gnathobases of marine planktonic copepods – feeding tools with complex micro- and nanoscale composite architectures. *Beilstein J. Nanotechnol.* 6, 674–685. doi: 10.3762/bjnano.6.68

Michels, J., Vogt, J., and Gorb, S. N. (2012). Tools for crushing diatoms - opal teeth in copepods feature a rubber-like bearing composed of resilin. *Sci. Rep.* 2:465. doi: 10.1038/srep00465

Miller, C. B., Nelson, D. M., Weiss, C., and Soeldner, A. H. (1990). Morphogenesis of opal teeth in calanoid copepods. *Mar. Biol.* 106, 91–101. doi: 10.1007/BF02114678

Nesbit, K. T., and Roer, R. D. (2016). Silicification of the medial tooth in the blue crab *Callinectes sapidus. J. Morphol.* 277, 1648–1660. doi: 10.1002/jmor.20614

Pierce, D. C., Butler, K. D., and Roer, R. D. (2001). Effects of exogenous N-acetylhexosamindase on the structure and mineralization of the postecdysial exoskeleton of the blue crab, *Callinectes sapidus. Comp. Biochem. Physiol.* 128B, 691–700. doi: 10.1016/S1096-4959(00)00362-6

Raabe, D., Romano, P., Sachs, C., Al-Sawalmih, A., Brokmeier, H.-G., Yi, S.-B., et al. (2005). Discovery of a honeycomb structure in the twisted plywood patterns of fibrous biological nanocomposite tissue. *J. Crystal Growth* 283, 1–7. doi: 10.1016/j.jcrysgro.2005.05.077

Rathbun, M. J. (1896). The genus *Callinectes. Proc. U.S. Nat. Mus.* 18, 349–375. doi: 10.5479/si.00963801.18-1070.349

Roer, R. D. (1980). Mechanisms of resorption and deposition of calcium in the carapace of the crab *Carcinus maenas. J. Exp. Biol.* 88, 205–218.

Roer, R. D., Abehsera, S., and Sagi, A. (2015). Exoskeletons across the Pancrustacea: a comparison of cuticular morphology, physiology, biochemistry and genetics between Decapoda and Hexapoda. *Integr. Comp. Biol.* 5, 771–791. doi: 10.1093/icb/icv080

Roer, R. D., Burgess, S. K., Miller, C. G., and Dail, M. B. (1988). "Control of calcium carbonate nucleation in pre- and postecdysial crab cuticle," in *Chemical Aspects of Regulation of Mineralization*, eds C. S. Sikes and A. P. Wheeler (Mobile, AL: Univ. of South Alabama Publication Service), 21–24.

Roer, R. D., and Dillaman, R. M. (1984). The structure and calcification of the crustacean cuticle. *Am. Zool.* 24, 893–909. doi: 10.1093/icb/24.4.893

Roer, R. D., and Dillaman, R. M. (1993). "Molt-related change in integumental structure and function," in *The Crustacean Integument - Morphology and Biochemistry*, eds M. Horst and J. A. Freeman (Boca Raton, FL: CRC Press), 1–37.

Roer, R. D., Halbrook, K. E., and Shafer, T. H. (2001). Glycosidase activity in the postecdysial cuticle of the blue crab, *Callinectes sapidus. Comp. Biochem. Physiol.* 128B, 683–690. doi: 10.1016/S1096-4959(00)00363-8

Roer, R., and Towle, D. (2004). Partial nucleotide sequence of a putative cuticular hexosaminidase from the blue crab, *Callinectes sapidus. MDIBL Bull.* 43, 40–42.

Roer, R., and Towle, D. (2005). Partial nucleotide sequence and expression of plasma membrane Ca-ATPase in the hypodermis of the blue crab, *Callinectes sapidus. MDIBL Bull.* 44, 40–43.

Shafer, T. H., Roer, R. D., Midgette-Luther, C., and Brookins, T. A. (1995). Postecdysial cuticle alteration in the blue crab, *Callinectes sapidus*: synchronous changes in glycoproteins and mineral nucleation. *J. Exp. Zool.* 271, 171–182. doi: 10.1002/jez.1402710303

Shafer, T. H., Roer, R. D., Miller, C. G., and Dillaman, R. M. (1994). Postecdysial changes in the protein and glycoprotein composition of the cuticle of the blue crab *Callinectes sapidus. J. Crust. Biol.* 14, 210–219. doi: 10.2307/1548901

Tweedie, E. P., Coblentz, F. E., and Shafer, T. H. (2004). Purification of a soluble glycoprotein from the uncalcified ecdysial cuticle of the blue crab *Callinectes sapidus* and its possible role in initial mineralization. *J. Exp. Biol.* 207, 2589–2598. doi: 10.1242/jeb.01070

Vatcher, H. E., Roer, R. D., and Dillaman, R. M. (2015). Structure and molt cycle dynamics of the dorsal ossicle complex in the gastric mill of the blue crab, *Callinectes sapidus*. *J. Morphol.* 276, 1358–1367. doi: 10.1002/jmor.20423

Williams, A., Lüter, C., and Cusack, M. (2001). The nature of siliceous mosaics forming the first shell of the brachiopod *Discinisca*. *J. Struct. Biol.* 134, 25–34. doi: 10.1006/jsbi.2001.4366